Supporting Information for

Connecting polymer synthesis and chemical recycling on a chain-by-chain basis: a unified matrix-based kinetic Monte Carlo strategy

Kyann De Smit,[a] Yoshi W. Marien,[a] Kevin M. Van Geem,[a] Paul H.M. Van Steenberge,[a] Dagmar R. D'hooge[a,b,*]

[a]Laboratory for Chemical Technology (LCT), Department of Materials, Textiles and Chemical Engineering, Ghent University, Technologiepark 125, 9052 Zwijnaarde, Belgium.

[b]Centre for Textile Science and Engineering (CTSE), Department of Materials, Textiles and Chemical Engineering, Ghent University, Technologiepark 70a, 9052 Zwijnaarde, Belgium.

[*]Corresponding author: dagmar.dhooge@ugent.be

1. Extra information on storage in *k*MC model

Figure S1 shows the flowsheet of the kMC model highlighting the overall steps of the algorithm. The basis is Gillespie's algorithm, which discretely samples reaction events based on the probabilities of the considered individual reaction types (e.g. initiation, propagation, termination, fission,...). These probabilities depend on intrinsic kinetic and diffusion parameters and the reactant concentrations. The algorithm is provided with initial reaction conditions at the start of the simulation (top left part of Figure S1). A MC volume sufficiently large to ensure numerical convergence is required as well. Also an initial time step needs to be stochastically sampled based on the total initial reaction rate.

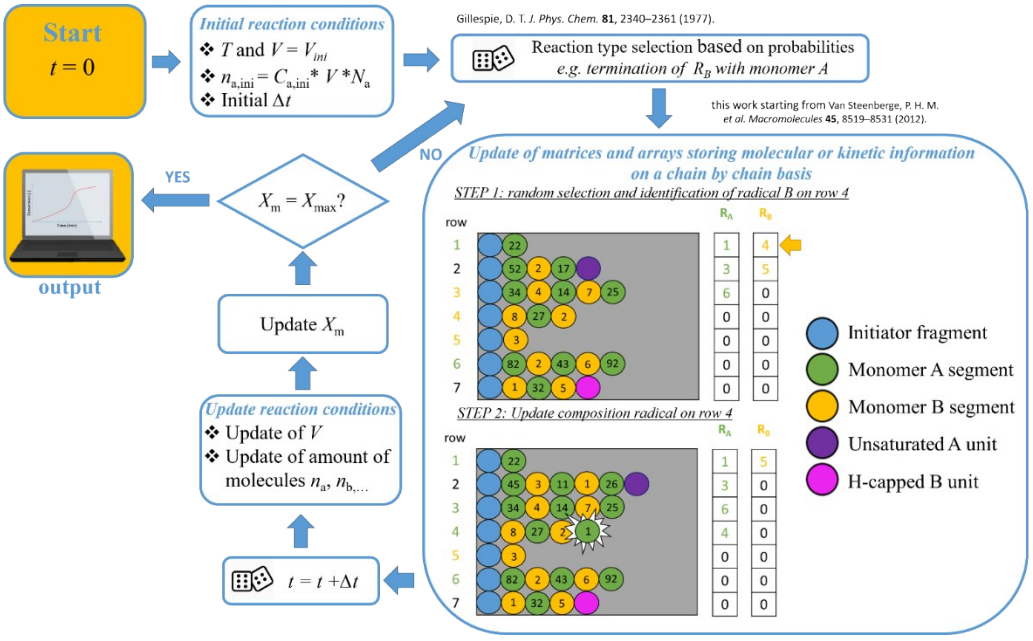

Figure S1: Flowsheet of t kinetic Monte Carlo (kMC) model for tracking detailed information on structural parameters/defects in individual (co)polymer chains as relevant for the synthesis and the subsequent degradation; comonomer types: A and B; Xm = monomer conversion: T: temperature; V: MC volume; C: concentration; n: number of moles; NA: Avogadro constant. The two extra columns allow to identify at which rows the macroradicals with either an active A or B and are located: RA and RB species.

The (initial) probabilities are then determined and the associated reaction event type is sampled based on these probabilities. For illustration purposes, in Figure S1, it is assumed that propagation is selected, more precisely a macrospecies with an active unit ending on B (R_B) is considered to take up one monomer A so that its active nature changes (R_A instead of R_B species). Thereafter, both the sequence and the segment length matrix (large box in Figure S1)

are updated to keep track of the variation of the individual molecular structure of all macrospecies. Note that two extra column arrays are used to enable a direct positioning of the active species in the sequence matrix distinguishing between R_A and R_B species. For other reaction types similar operations are needed. For termination two radicals need to be selected by two random numbers instead one as is the case for propagation.

After the execution of each reaction event the overall state of the system is updated to enable a further repetition of the previous steps (left bottom part of Figure S1). This mainly comprises an update of the reaction time for the next reaction, the (overall) monomer conversion X_m, the number of molecules and concentrations, and the MC volume. Once X_m exceeds a predetermined value, the program exits and the most important molecular characteristics are processed via tailored output facilities. Here we can opt to plot conventional concentration variations or depict a chain length or MMD or even the explicit molecular structure of an ensemble of individual chains.

Figure S2 is an expansion of Figure S1, highlighting more in detail the storage facilities. An important thing to note is that for a rather large reaction volume the main matrix becomes very large. It is very time consuming to check the whole main matrix each reaction event for the nature of the macromolecule on a specific row. For example, if we want to find the first 5 radicals in the main sequence matrix, we would have to check every single row for the possibility of a macroradical. This is very inefficient and to tackle this issue we introduced extra vectors which keep track of all the radicals of type A and B. Extra vectors can of course be added for other macromolecular reactants, which are stored in the main matrix. In Figure S1, it is shown why our data structure is much more efficient in storing large macromolecules, especially with the maximum RAM-memory usage in mind (32 GB), thus increasing the possible reaction volume.

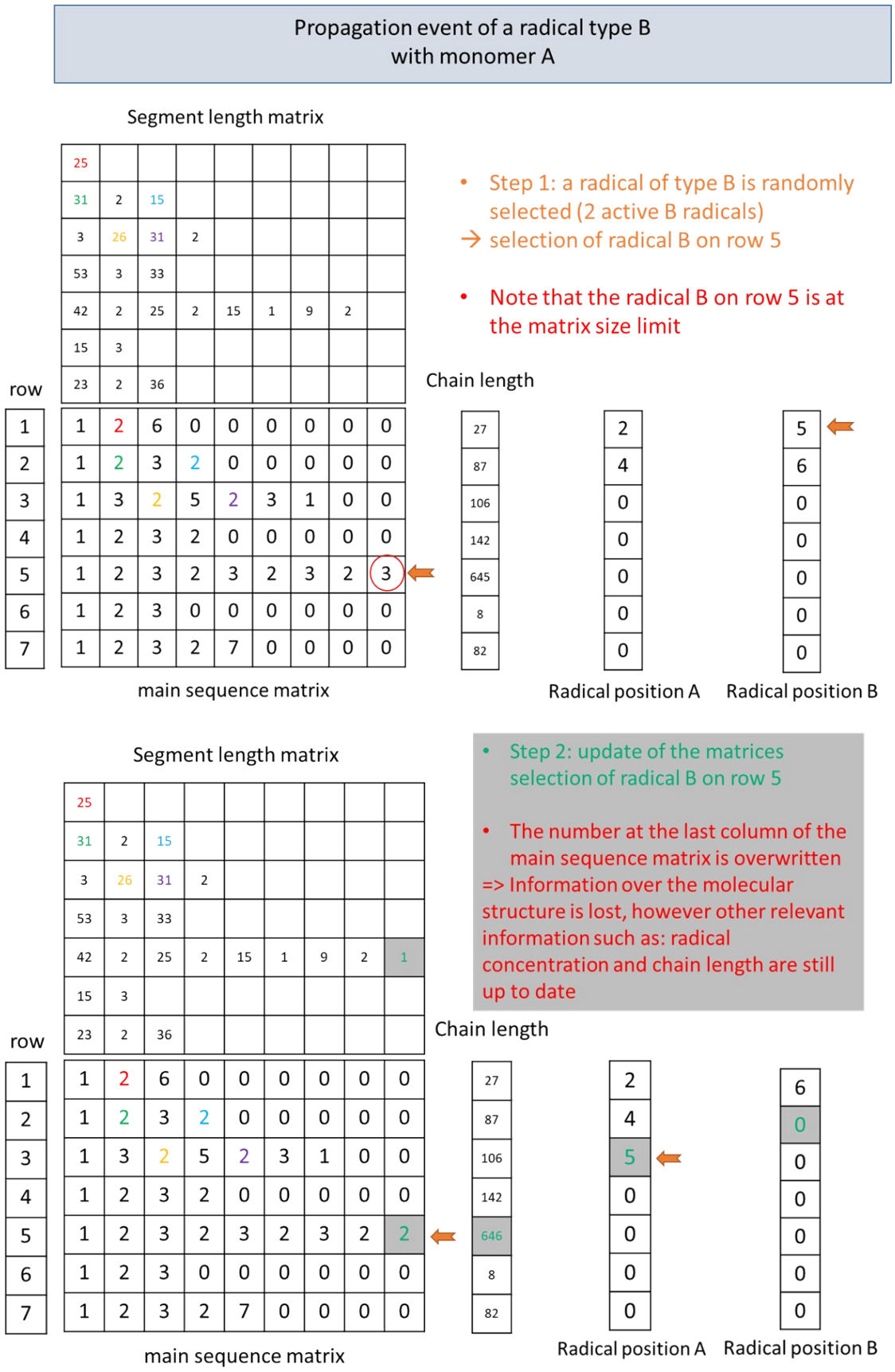

Figure S2: More detailed explanation of the principles laid out in Figure 2 in the main text. Example of reaction at which the last element in the main sequence matrix is reached.

For the copolymerization, the problem of memory usage at larger reaction volumes is even more critical; the amount of columns necessary to store the larger copolymer chains of a more alternating nature is specifically expected. Because of this we are obliged to limit the array size to a set value. If a chain threatens to exit the main matrix because of its size, the last element is overwritten. This means we still respect the mass balances of the system, while losing information over the molecular information of the largest copolymer chains. In practice, this has a very minimal effect on the average properties and thus, this is an elegant way of dealing with the computer memory limit.

2. Reaction mechanism FRP of MMA

Figure S3 gives the FRP reaction scheme for MMA as considered in the main manuscript. Note that the chain initiation reaction by a monomeric radical, formed through the chain transfer to monomer, results in the formation of a chain starting with an unsaturation. This resembles a chain which is formed through the disproportionation reaction. Even though chain transfer to monomer is rather rare in the free radical polymerization of MMA, the formation of these unsaturations is still important for the prediction of the mass loss during degradation as they present a weak moiety in the PMMA chain.

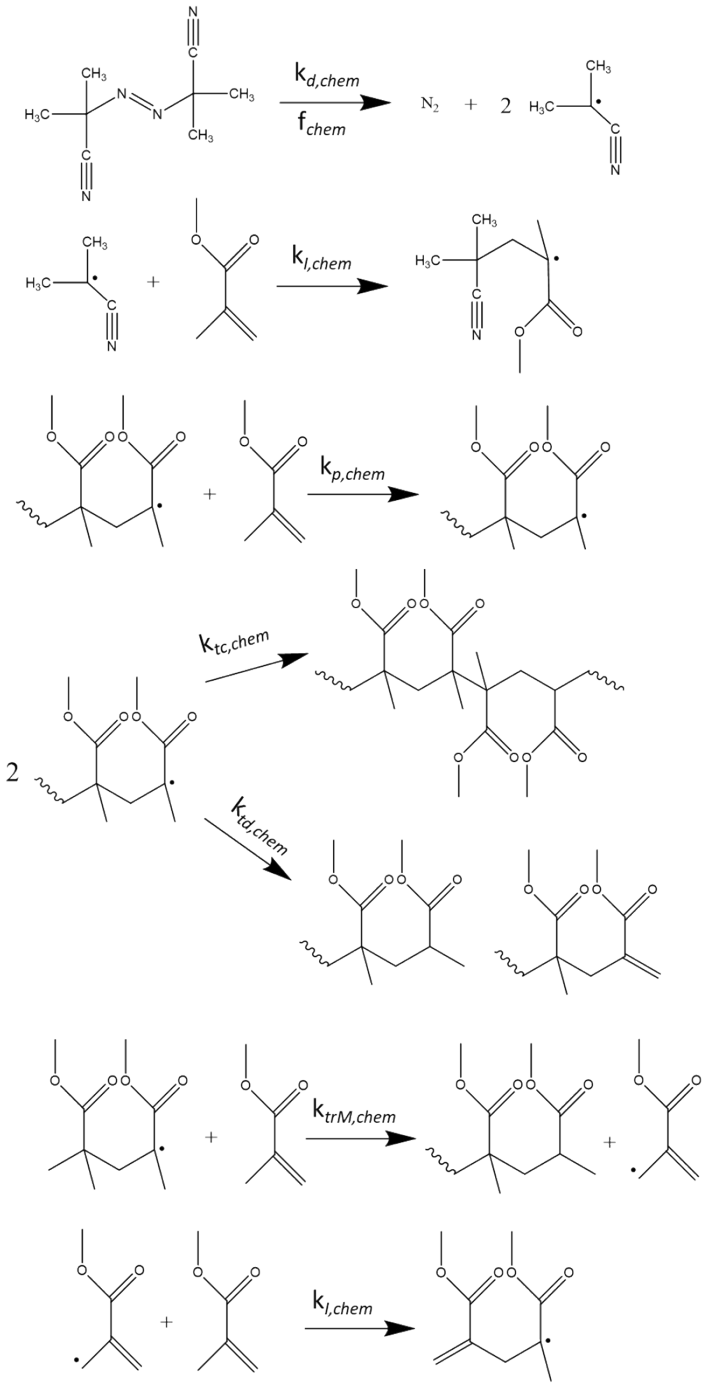

Figure S3: Reaction scheme free radical polymerization of MMA. Here all rate coefficients are chemical intrinsic ones.

3. Simulation of diffusional limitations on main reactions in free radical polymerizations

3.1 The gel effect: RAFT-CLD-T method

Apparent "homo-termination" rate coefficients (equal chain lengths) as determined with the so-called composite k_t or RAFT-CLD-T model are used to calculation chain length and polymer mass fraction (w_p) dependent apparent termination rate coefficients. Since bulk free radical polymerization of MMA is modeled, w_p can be taken equal to the monomer conversion. The corresponding equations are given below[1]:

$$for\ i < i_{gel}\ and\ i < i_{SL}: k_{t,ii}^{app} = k_{t,11}^{app} i^{-\alpha_s} \qquad (S1)$$

$$for\ i < i_{gel}\ and\ i \geq i_{SL}: k_{t,ii}^{app} = k_{t,11}^{app} i_{SL}^{\alpha_l - \alpha_s} i^{-\alpha_l} \qquad (S2)$$

$$for\ i \geq i_{gel}\ and\ i < i_{SL}: k_{t,ii}^{app} = k_{t,11}^{app} i_{gel}^{\alpha_{gel} - \alpha_s} i^{-\alpha_{gel}} \qquad (S3)$$

$$for\ i \geq i_{gel}\ and\ i < i_{SL}: k_{t,ii}^{app} = k_{t,11}^{app} i_{SL}^{\alpha_l - \alpha_s} i_{gel}^{\alpha_{gel} - \alpha_l} i^{-\alpha_{gel}} \qquad (S4)$$

in which $k_{t,11}^{app}$ is the termination rate coefficient for radicals with a chain length 1, α_s the exponent for termination of short chains in dilute solution, α_L the exponent for long chains in dilute solution, α_{gel} the exponent for chain in the gel regime, i_{SL} the chain length between short- and long-chain behaviour, and i_{gel} the chain length at the onset of the gel-effect.

The apparent "cross-termination" rate coefficient for each radical chain length combination is then calculated by taking the geometric mean of the two apparent homotermination coefficients[1,2]:

$$k_{t,app}^{ij} = \sqrt{k_{t,app}^{ii} k_{t,app}^{jj}} \qquad (S5)$$

The corresponding average thus becomes:

$$\langle k_{t,app} \rangle = \sum_i \frac{\sum_j k_{t,app}^{ij} R_i R_j}{\left(\sum_i R_i\right)^2} \qquad (S6)$$

The apparent rate coefficients by termination by recombination and disproportionation are always obtained upon taking the appropriate fraction in the main text.

3.2.Glass effect: parallel encounter pair model

The glass effect is modeled using the parallel encounter pair model that calculates in principle chain length dependent apparent propagation rate coefficients ($k^i_{p,app}$ values):[3]

$$\frac{1}{k_{p,app}^{\ i}} = \frac{1}{k_{p,chem}^{\ i}} + \frac{1}{k_{p,diff}^{\ i}} \qquad (S7)$$

in which $k^i_{p,chem}$ is the intrinsic rate coefficient for the propagation reaction (with chain length i), $k^i_{p,diff}$ is the corresponding diffusion rate coefficient which is a measure for the rate at which the two species diffuse toward each other. This contribution is calculated using the Smoluchowski model with the mutual diffusion coefficient approximated by the translational diffusion coefficient of the monomer[4,5]:

$$k_{p,diff}^{\ i} = k_{p,diff} = 4\pi\sigma_p N_A D_{tr,M} \qquad (S8)$$

Here σ_p is the propagation reaction distance, N_A the Avogadro number and $D_{tr,M}$ is the translational diffusion coefficient of the monomer. In practice, intrinsic chain length dependencies are also less relevant in a FRP process and, hence, a chain length independent apparent propagation rate coefficient can be employed.

Table S1: Parameters to enable the calculation of the apparent propagation rate coefficient.

Parameter	Description	Value[6–8]
$D_{M,0}\ (m^2 s^{-1})$	Pre-exponential factor for diffusion	$1.27\ 10^{-7}$
$E_{a,M}\ (kJ\ mol^{-1})$	Activation energy for diffusion	$12\ (\geq 323K)$ $and\ 23.5\ (<323K)$
$R\ (J\ mol^{-1}K^{-1})$	Universal gas constant	8.314
$T\ (K)$	Temperature	323 – 363
$w_m\ (-)$	Mass fraction of monomer	0-1
$w_p\ (-)$	Mass fraction of polymer	0-1
$V_m^*\ (m^3 kg^{-1})$	Specific critical hole free volume of monomer	$0.872\ 10^{-3}$
$K_{1,M}\ (m^3\ kg^{-1}\ K^{-1})$	Parameter for specific hole free volume polymer	$6.91\ 10^{-7}$
$K_{1,p}\ (m^3\ kg^{-1}\ K^{-1})$	Parameter for specific hole free volume polymer	$2.92\ 10^{-7}$
$K_{2,M} - T_{g,M}\ (K)$	Parameter for specific hole free volume monomer	72.26
$K_{2,p} - T_{g,p}\ (K)$	Parameter for specific hole free volume polymer	– 250.21
$M_{j,M}\ (g\ mol^{-1})$	Molar mass monomer	100.1

$D_{\mathrm{tr,M}}$ is calculated using the free volume theory[4,5]:

$$D_{tr,M} = D_{M,0}\, e^{-\frac{E_{a,M}}{RT}\left(-V_M^* M_{j,M} \frac{\frac{w_m}{M_{j,M}} + \frac{w_p}{M_{j,M}}}{V_{FH}/\lambda}\right)}$$

with $$\frac{V_{FH}}{\lambda} = w_m \frac{V_{FH,M}}{\lambda_M} + w_p \frac{V_{FH,p}}{\lambda_p}$$

and $$\frac{V_{FH,A}}{\lambda_A} = K_{1,A}\left(K_{2,A} - T_{g,A} + T\right)$$

The relevant parameters are found in Table S1 together with a description of their physical meaning.

Cage effect: apparent initiator efficiency

The evolution of the apparent initiator efficiency f_{app} with increasing monomer conversion is taken from the work of Buback *et al.*:[9]

$$f_{app} = \frac{D_I}{D_I + D_{term}} \qquad (S9)$$

in which D_I is the diffusion coefficient of the cyanoisopropyl radical and D_{term} a correction factor, related to the rate of termination between two cyanoisopropyl radicals. Buback only reported this value for 343K (5.3 10^{-10} $m^2 s^{-1}$). Since the present work highlights lower termination rates at lower temperatures in general we changed this value for the lower temperatures (cf. classification in Table 2 in the main text) to 4.8 10^{-10} $m^2 s^{-1}$. The free volume theory is used to obtained D_I at a given temperature and reaction mixture composition:

$$D_I = D_{0,I}\, e^{-\frac{E_{a,I}}{RT}\left(-\frac{w_m V^*_m \xi_{cp}/\xi_{mp} + w_p V^*_p \xi_{cp}}{V_{FH}/\lambda}\right)} \qquad (S10)$$

$$\frac{V_{FH}}{\lambda} = \frac{K_{mm}}{\lambda} w_m (K_{mp} - T - T_{g1}) + \frac{k_{mp}}{\lambda} w_p (K_{pp} + T - T_{g1}) \qquad (S11)$$

with D_I the diffusion coefficient for the cyanoisopropyl radical, $D_{0,I}$ the pre-exponential factor, $E_{a,I}$ the energy per mole that a cyanoisopropyl radical needs to overcome attractive forces which hold it to its neighbours, w_x the mass fraction of monomer $(x = m)$ or polymer $(x = p)$, V^*_x the specific volume of the monomer $(x = m)$ or the polymer $(x = p)$, ξ_{xy} is the ratio of the critical molar volume of the cyanoispropyl radical $(x = c)$ or monomer $(x = m)$ compared to the polymer $(y = p)$, and V_{FH}/λ is related to the total free volume. Table S2 gives an overview of the related parameters (AIBN/styrene system but sufficiently representative).

Table S3: Parameters to enable the calculation of the apparent propagation rate coefficient.

Parameter	Description	Value[6,7,9]
$D_{0,I}\,(m^2 s^{-1})$	Pre-exponential factor for diffusion	$1.87\ 10^{-8}$
$E_I\,(kJ\ mol^{-1})$	Activation energy for diffusion	7.10 (a)
$R\,(J\ mol^{-1}K^{-1})$	Universal gas constant	8.314
$T\,(K)$	Temperature	323 – 363
$w_m\,(-)$	Mass fraction of monomer	0-1
$w_p\,(-)$	Mass fraction of polymer	0-1
$V_m^*\,(m^3 mol^{-1})$	Specific critical hole free volume of monomer	$0.822\ 10^{-6}$
$V_p^*\,(m^3 kg^{-1})$	Specific critical hole free volume of polystyrene	$0.77\ 10^{-6}$
$\frac{K_{mm}}{\lambda}\,(m^3\ kg^{-1}\ K^{-1})$	Parameter for specific hole free volume monomer	$1.49\ 10^{-9}$
$\frac{K_{mp}}{\lambda}\,(m^3\ kg^{-1}\ K^{-1})$	Parameter for specific hole free volume polymer	$5.82\ 10^{-10}$
$K_{pm} - T_{g1}\,(K)$	Parameter for specific hole free volume monomer	72.26
$K_{pp} - T_{g1}\,(K)$	Parameter for specific hole free volume polymer	– 250.21
$\xi_{cp}\,(-)$	Critical jumping unit volume ratio for cyanoispropyl radical to polymer	0.537
$\xi_{mp}\,(-)$	Critical jumping unit volume ratio for monomer to polymer	0.712

[a] values are slightly adjusted in order to improve description of experimental data.

4. Free radical polymerization of MMA: extra simulated information

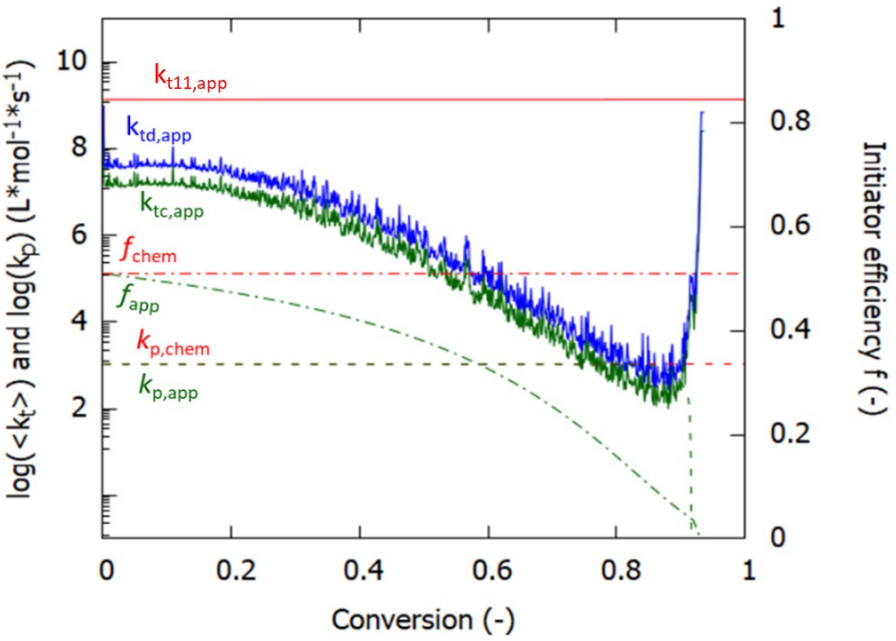

Figure S4: Extra information for Figure 6 (343 K) in the main text with green lines the apparent rate coefficients; apparent termination rate coefficient shown for both recombination (green line) and disproportionation (blue line); and the red lines: "intrinsic chemical" rate coefficients/efficiency; the full lines give the termination rate coefficients, the dashed lines show the propagation rate coefficients and the dashed-dotted line shows the initiator efficiencies as a function of the monomer conversion.

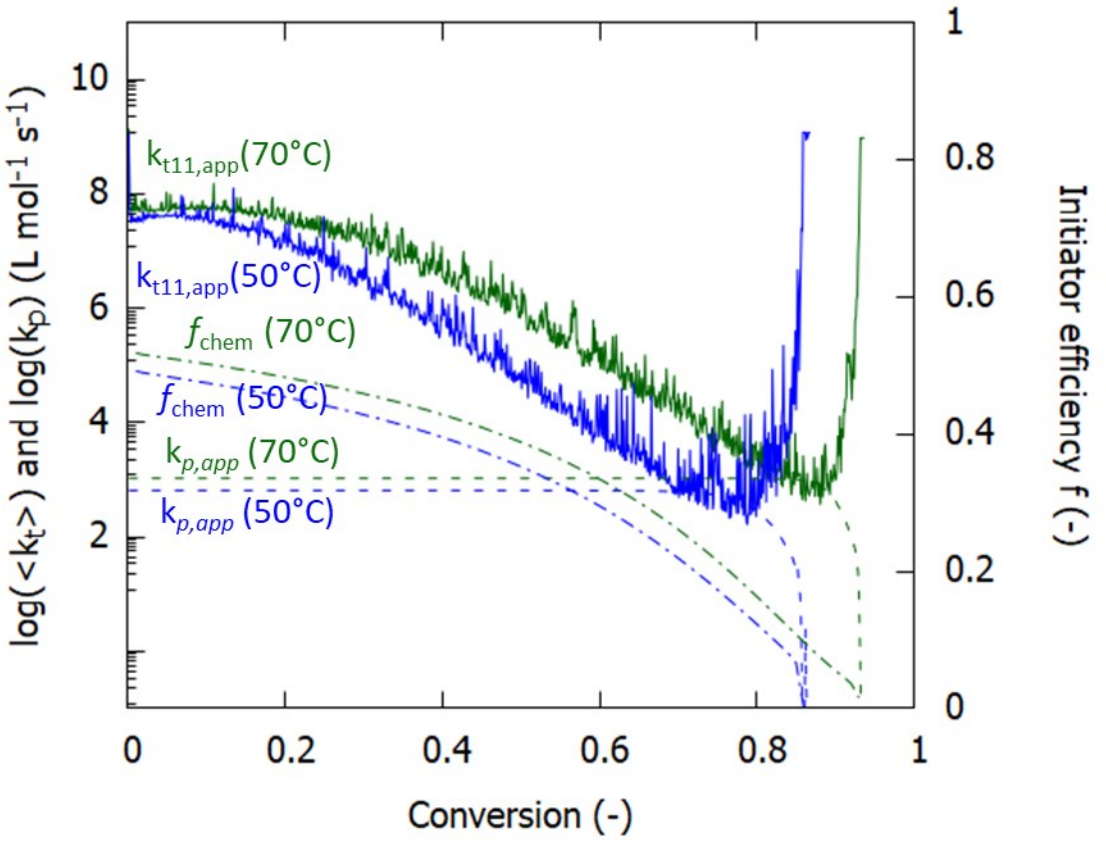

Figure S5: Update of previous figure focusing at 323K (blue lines) and 343 K (green lines); related to Figure 7 in the main text).

5. Synthesis and thermal degradation of PMMA: extra simulated information

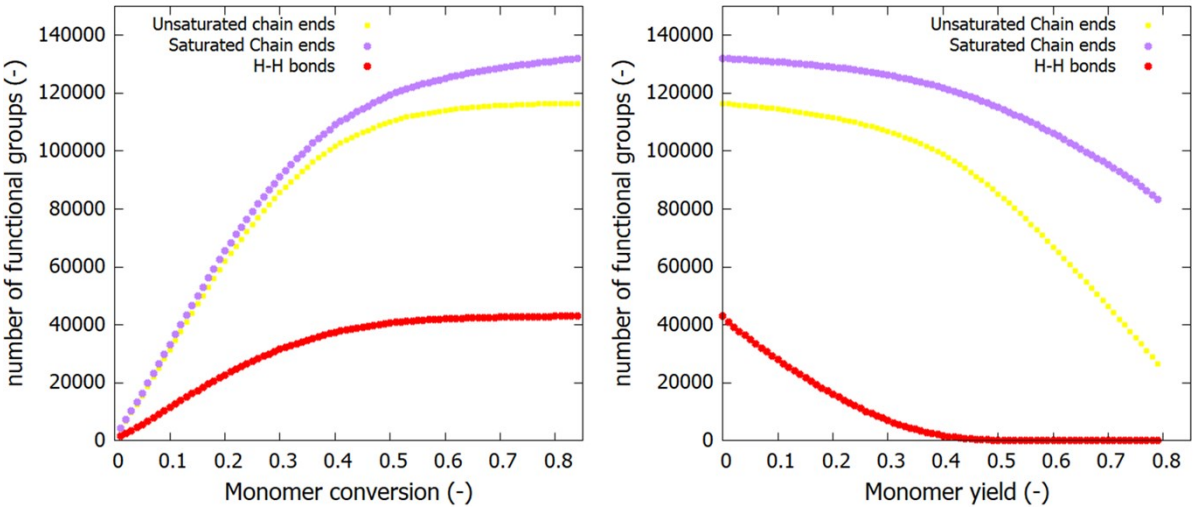

Figure S6: Evolution of the number of functional groups/defects both during polymerization (left) and degradation (right). Note that the amount of these functional groups/defects is given in absolute numbers and not in concentrations due to the volume changes during the polymerization and degradation. The numbers are sufficiently high to enable correct sampling for both steps.

6. Free radical copolymerization of MMA and MDO: extra simulated information

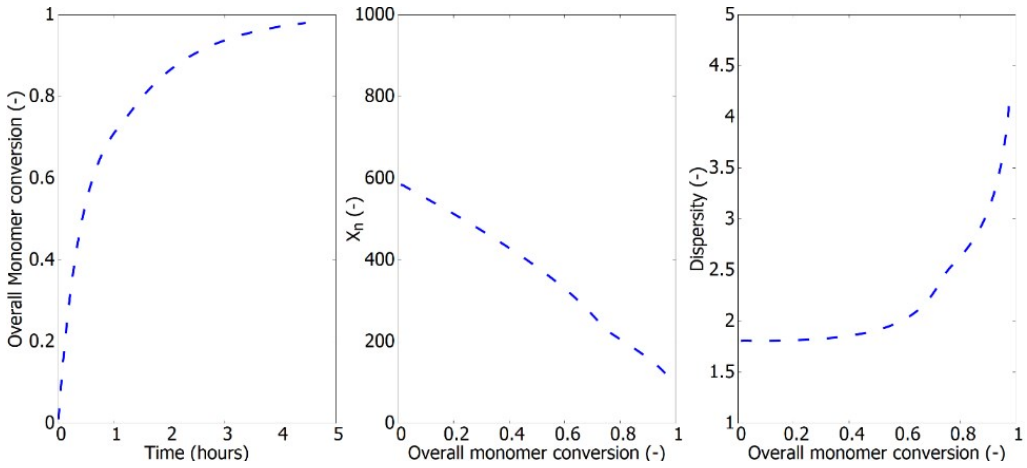

Figure S7: Extra characteristics compared to Figure 7 (343 K; free radical copolymerization of MMA and MDO with $f_{MMA,0}$= $f_{MDO,0}$ = 0.5.) in the main text: left: the overall monomer conversion profile middle: the number average chain length x_n as a function of the overall monomer conversion and right: the dispersity as a function of the overall monomer conversion.

The average length of MMA segments in the MMA/MDO copolymer is given by:

$$\bar{l}_{MMA,inst} = \frac{1}{p_{MMA/MDO}} \qquad (S12)$$

with $p_{MMA/MDO} = \frac{f_{MDO}}{r_{MMA} f_{MMA} + f_{MDO}}$ being the probability that a radical with a terminal MMA unit propagates with a MDO monomer, f_{MDO} the MDO feed fraction, r_{MMA} the reactivity ratio for MMA with respect to MDO and f_{MMA} the MMA feed fraction. For the average length of MDO segments one just needs to swap between MDO and MMA in the formula. Some examples of simulated segment length distributions are provided in Figure S7.

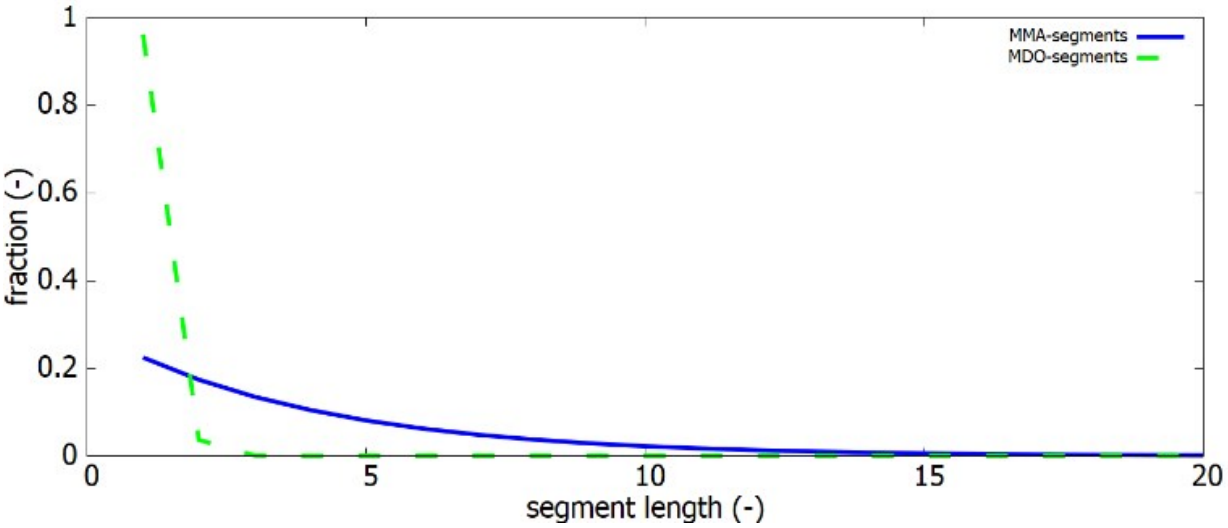

Figure S8: Examples of segment length distributions at 1% overall monomer conversion as obtainable by the kMC model. Same conditions as in main text

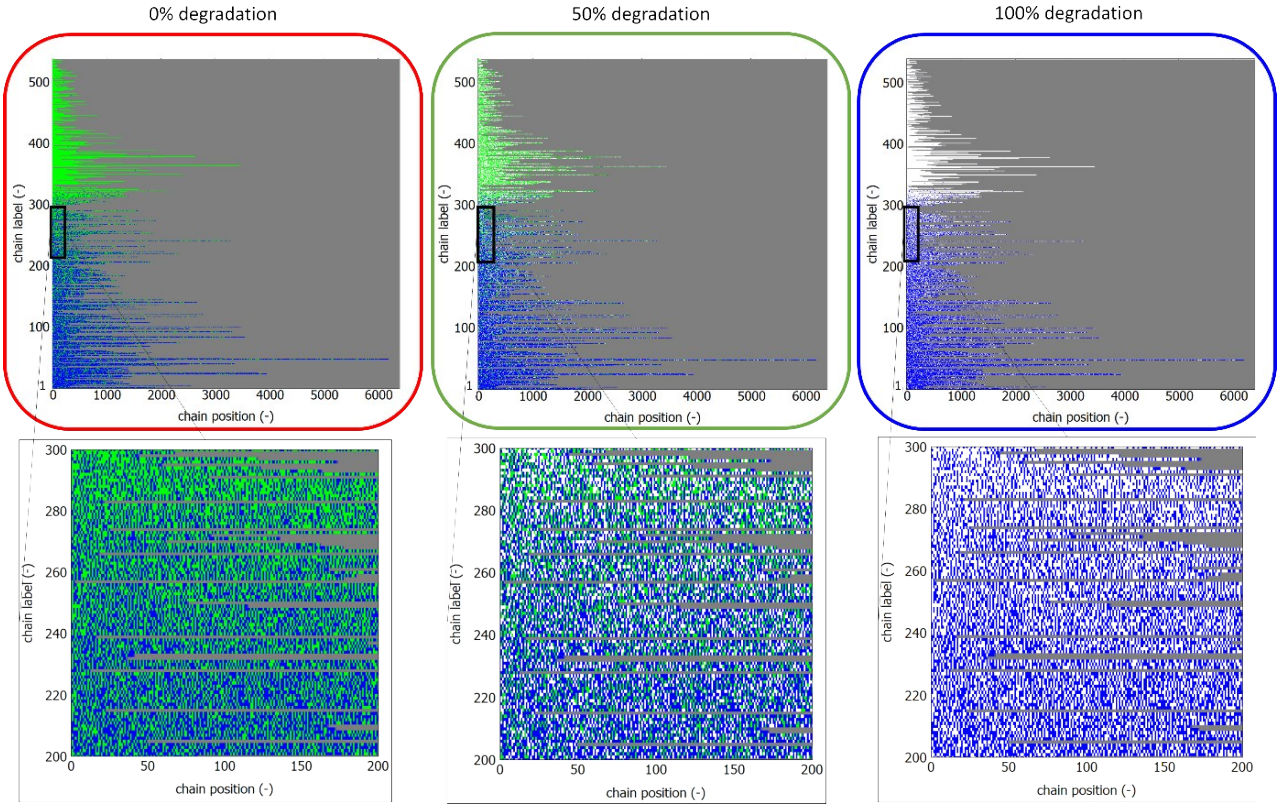

Figure S9: Visualization of degradation of poly(MMA-MDO) from batch radical copolymerization at 343 K with 2 mol% AIBN initially and equimolar feed of MMA and MDO, via hydrolysis; red box: poly(MMA-MDO) copolymer after polymerization (same as Figure 11(b)); green box: poly(MMA-MDO) copolymer with 50% of ester linkages being hydrolyzed; blue box: fully degraded poly(MMA-MDO); MMA/MDO segments in blue/green; degraded MDO unit: white; original background: grey.

7. References

1 G. Johnston-Hall and M. J. Monteiro, *Prog. Polym. Sci.*, 2008, **46**, 936–946.

2 P. Derboven, D. R. D'hooge, M.-F. Reyniers, G. B. Marin and C. Barner-Kowollik, *Macromolecules*, 2015, **48**, 492–501.

3 D. R. D'hooge, M. F. Reyniers and G. B. Marin, *Macromol. React. Eng.*, 2013, **7**, 362–379.

4 J. S. Vrentas and J. L. Duda, *J Polym Sci Polym Phys Ed*, 1977, **15**, 403–416.

5 J. S. Vrentas, J. L. Duda and H. C. Ling, *J. Polym. Sci. Part A-2, Polym. Phys.*, 1984, **22**, 459–469.

6 D. R. D'hooge, M.-F. Reyniers and G. B. Marin, *Macromol. React. Eng.*, 2009, **3**, 185–209.

7 D. S. Achilias and C. Kiparissides, *Macromolecules*, 1992, **25**, 3739–3750.

8 D. S. Achilias, *Macromol. Theory Simulations*, 2007, **16**, 319–347.

9 M. Buback, B. Huckestein, F. -D Kuchta, G. T. Russell and E. Schmid, *Macromol. Chem. Phys.*, 1994, **195**, 2117–2140.